New Algorithms for Widefield SAR Image Formation

Walter G. Carrara, Ron S. Goodman, and Mark A. Ricoy
General Dynamics Advanced Information Systems
P.O. Box 134008
Ann Arbor, MI 48113-4008 USA

Abstract: **The widefield polar format algorithm, the Stolt polar algorithm, and the differential Doppler algorithm use variations of a new along-track alignment and formatting system (ATAFS) to generate fine-resolution images from synthetic aperture radar (SAR) data. ATAFS introduces a spatially-variant modification of the SAR phase history storage format to remove the formatting inaccuracies of the conventional polar format algorithm and enable full image quality over large scenes without range curvature distortion or image defocus.**

These new algorithms are well-suited for processing fine resolution spotlight and ultra-wideband SAR data. Their image quality performance is comparable to that of the range migration algorithm (RMA). Unlike RMA, the new algorithms operate on data stabilized to a fixed reference point to remove the azimuth chirp (the Doppler bandwidth of the reference point) before it compromises processor efficiency.

I. INTRODUCTION

Modern synthetic aperture radar (SAR) missions demand both fine spatial resolution and large processed scene size. In a mission requiring coherent exploitation of SAR imagery, such as interferometric SAR, it is highly desirable that the SAR processor yield images free of amplitude and phase discontinuities. The need for large seamless images at fine resolution can present difficult challenges to a SAR image formation algorithm.

The SAR community has developed a number of image formation algorithms to meet these challenges. Each algorithm possesses unique capabilities and limitations that determine its applicability for specific SAR systems and missions. The polar format algorithm (PFA) is a common choice for producing fine resolution imagery from SAR data collected in the spotlight mode. The popularity of PFA stems from its simplicity, its ability to address a number of real-world SAR system requirements such as 3-D motion compensation, and its modest computational burden. However, the presence of range curvature quadratic phase error (RCQPE) in PFA imagery limits maximum useful scene size. RCQPE is a spatially variant effect that increases in severity with scatterer distance from scene center. Its spatial variance makes RCQPE difficult and expensive to compensate in the complex image generated by a PFA processor.

Because it does not suffer RCQPE, the range migration algorithm (RMA) [1] is potentially an ideal choice for fine-resolution SAR imaging of large scenes in challenging environments. However, RMA operates on phase history data containing the full Doppler bandwidth or azimuth chirp introduced by the data collection geometry. The high along-track sampling rate needed to maintain this azimuth chirp degrades RMA computational efficiency, particularly in long-range, fine-resolution spotlight mode.

Unlike RMA, the new algorithms operate on radar data with stabilization to a fixed point that removes the natural azimuth chirp before it degrades processor efficiency. Like RMA, they are widefield algorithms in that they do not degrade image focus away from scene center. The new algorithms produce imagery that is mathematically equivalent to RMA. In certain imaging applications, they can offer the computational advantage of PFA with the image quality of RMA.

II. DATA FORMAT PERSPECTIVE

Data formatting is a critical element in a fine-resolution SAR image formation processor. Its objective is to establish the incoming phase history data in an orthogonal wavenumber or spatial frequency domain (K_X, K_Y) such that a 2-D Fourier transform yields undistorted diffraction-limited imagery of 3-D scenes. A rectangular format algorithm, the PFA, and the RMA offer a progression from a simple format to an ideal format; from limited scene size and image quality to large seamless images at excellent image quality; and from minimum computational cost to possibly excessive computational burden.

Fig. 1 illustrates the ideal data format for targets at scene center, offset in range, and offset in azimuth during a broadside data collection in spotlight mode. It illustrates data support and format by showing the location of radar returns from the first P_{first}, middle P_{mid}, and last P_{last} transmitted pulses in raw collected data and in an ideal data format. Each linear FM transmitted pulse has bandwidth extending from low frequency f_{low} to high frequency f_{high}. Each scatterer in the collected data possesses the same support in pulse interval (radar along-track position X). After range deskew [2], each scatterer also has common support in radial frequency K_R which is related to transmitted frequency f by $K_R = 4\pi f / c$. Fig. 1a shows that a scene center target is viewed over a Doppler cone angle α_{dc} interval centered on $\alpha_{dc} = 90$ deg during a data collection interval from pulses P_{first} to P_{last}. For the same pulses, Fig. 1b shows that a target at far range is viewed over a narrower cone angle α_{dr} interval centered on $\alpha_{dr} = 90$ deg. Similarly, Fig. 1c shows that a target offset in azimuth is viewed over a cone angle α_{da} interval comparable to the scene center target but offset from 90 deg. The ideal format for each target reflects these differences in observed cone angle α_d and corresponding Doppler frequency f_d given by $f_d = 2\,V_a f \cos(\alpha_d) / c$ where V_a is the radar along-track velocity. The related azimuth spatial frequency is given by $K_X = -4\pi f \cos(\alpha_d) / c$ [2]. RMA and the new algorithms presented here achieve the ideal format for all scatterers while PFA fails to do so for targets away from scene center.
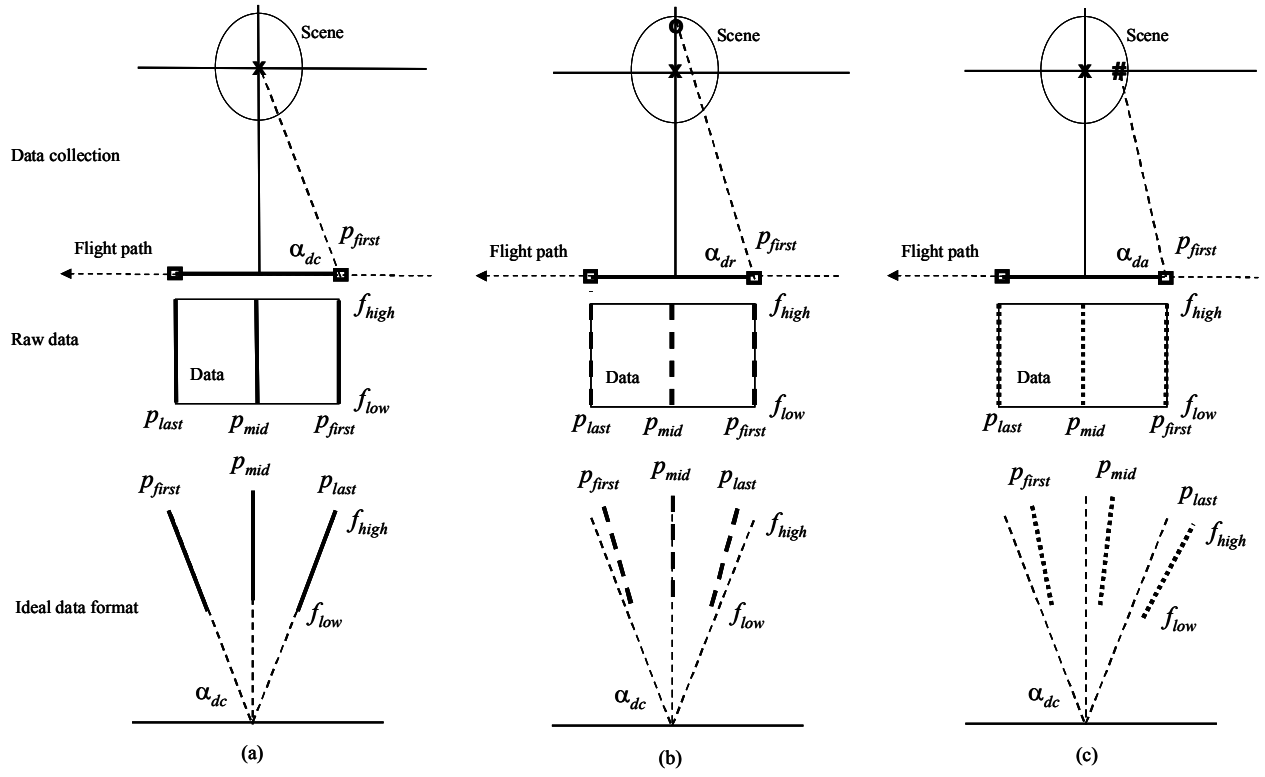
Fig. 1. Data collection and ideal data formats. (a) Scene center target **x**. (b) Far range target **o**. (c) Right azimuth target **#**.

PFA modifies the phase history format with a change in variables from rectangular (X by K_R) to polar (cone angle to scene center α_{dc} by K_R). However, only a scatterer at scene center receives the ideal format. Scatterers at other locations reside at different cone angles during a specific pulse, but PFA erroneously formats them to the cone angle of the scene center scatterer. In fact, a scene center target and one offset only in azimuth have similar but offset angular intervals while a more-distant target has a narrower angular interval. Fig. 2 shows this formatting inaccuracy by comparing the formatting of different targets before and after polar format to the ideal format. This formatting inaccuracy causes geometric distortion and defocusing in the PFA image that limit useful scene size.

III. ALONG-TRACK ALIGNMENT AND FORMATTING SYSTEM

The key to the new widefield algorithms is a processing stage which we call the along track alignment and formatting

system (ATAFS). ATAFS operates on SAR phase history data collected using a linear FM waveform after range dechirp and after a number of preprocessing operations associated with fine resolution SAR image formation that are common to all image formation algorithms. Fig. 3 summarizes these operations that may include motion compensation, azimuth presumming, range deskew, waveform correction, and compensation for a nonplanar data collection surface [2]. Following these operations, a data stabilization function beyond compensation for unplanned antenna motions differs significantly among the algorithms we discuss. A variation in data stabilization relative to current image formation algorithms is basic to the ATAFS and to the new algorithms that it motivates.

Fig. 4 shows the signal flow for ATAFS and for the individual widefield algorithms. Two ATAFS configurations (one associated with WPFA and SPA and another associated with DDA) differ in the nature of the phase adjustments in the
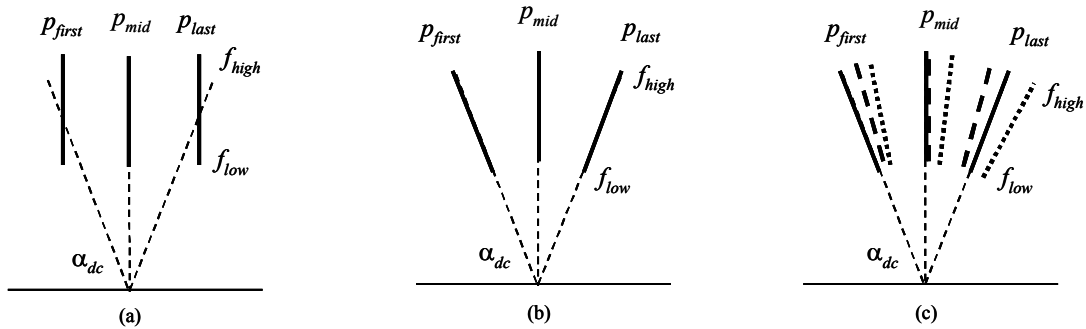

Fig. 2. Illustration of actual and ideal data formats with solid line = scene center returns, dashes = range offset target returns, and dots = azimuth offset target returns. (a) Raw data where all target returns coincide. (b) PFA storage format where all target returns coincide. (c) Ideal data storage format.
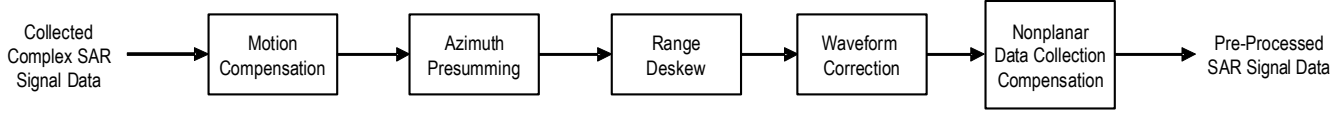
Fig. 3. Typical SAR preprocessing operations.

series of operations in Fig. 4a. Following ATAFS processing, WPFA proceeds with a change of angular variable (which does not require interpolation) and the conventional PFA algorithm in Fig. 4b. In the SPA variation of WPFA in Fig. 4c, ATAFS feeds into an azimuth reformatting stage followed by the well-known Stolt interpolation [3] associated with RMA. Following ATAFS and an azimuth parameter scaling operation, DDA proceeds with conventional Stolt interpolation to achieve proper range formatting in Fig. 4d. In each case, image formation concludes with a two-dimensional Fourier transform to generate a complex image from the two-dimensional spatial frequency data.

The new algorithms differ from RMA and PFA primarily in the azimuth channel. Taking the liberty in the PFA signal flow to perform the azimuth polar interpolation separately from and before the range polar interpolation, the WPFA, SPA, DDA, RMA, and this rearranged PFA have identical range processing stages equal to Stolt interpolation. The WPFA, SPA, DDA, and RMA achieve identical azimuth formatting by different implementations; each implementation is theoretically superior to the PFA approach. They properly migrate and expand the data in azimuth to account completely for range curvature after subsequent range processing.

Fig. 5 compares the azimuth signal flows for DDA, RMA, and PFA. The first operation for each algorithm requires application of a phase adjustment to the preprocessed SAR data. In Fig. 5b, RMA uses this adjustment to achieve data stabilization to a line and preserve the azimuth chirp

characteristic of the received data. In RMA, an along-track Fourier transform follows the first phase multiply. A second phase multiply incorporates a matched filter to remove the azimuth chirp and complete the azimuth processing.

In Fig. 5c, PFA begins with data stabilization to a point that eliminates the azimuth chirp from the phase history. This process also eliminates range curvature phase effects from the reference point (scene center). PFA then proceeds with azimuth interpolation to achieve the chosen azimuth format.

Three key aspects of ATAFS are: 1) the division of data stabilization to a point into two distinct operations, 2) the along-track (or slow-time) migration of the data support of targets as a function of their along-track location, and 3) the along-track scaling of the data support of targets as a function of their range location. This process requires an extra phase multiply and azimuth Fourier transform not present in the RMA signal flow. Like RMA, the DDA implementation achieves the proper azimuth format without the need for azimuth interpolation while both WPFA and SPA require azimuth interpolation after ATAFS.

To illustrate these ATAFS operations, we examine three point targets within a spotlight scene illustrated in Fig. 6a. Point A is located at scene center, point B is offset in range, and point C is offset in azimuth. Phase history data from these point targets proceed through ATAFS differently for WPFA (and SPA) and for DDA because of differences in the phase multiply operations.
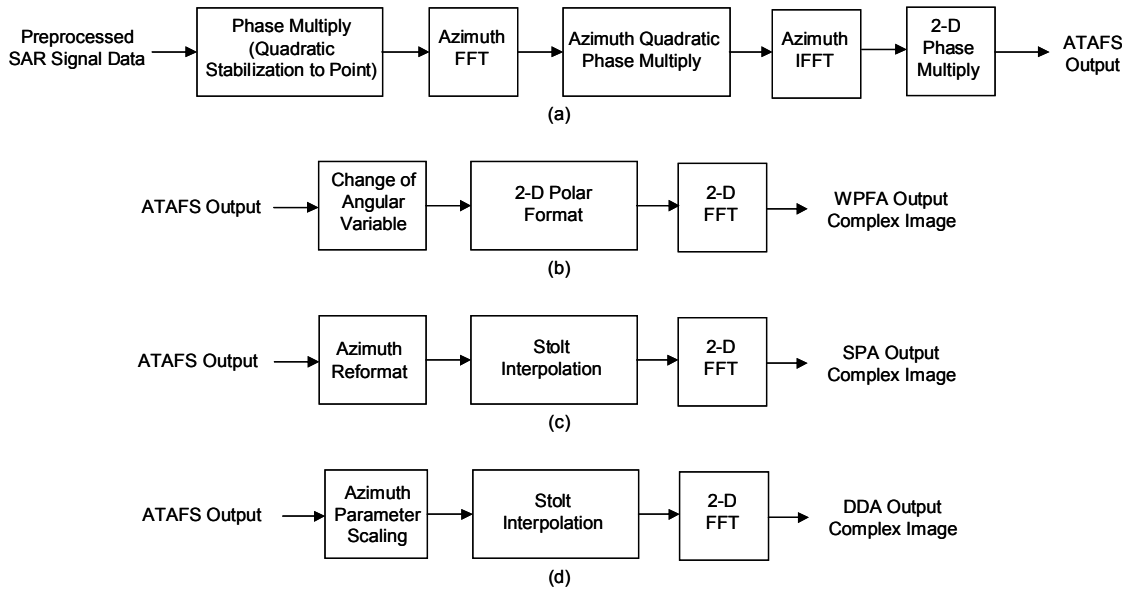

Fig. 4. Signal flows. (a) ATAFS. (b) WPFA after ATAFS. (c) SPA after ATAFS. (d) DDA after ATAFS.
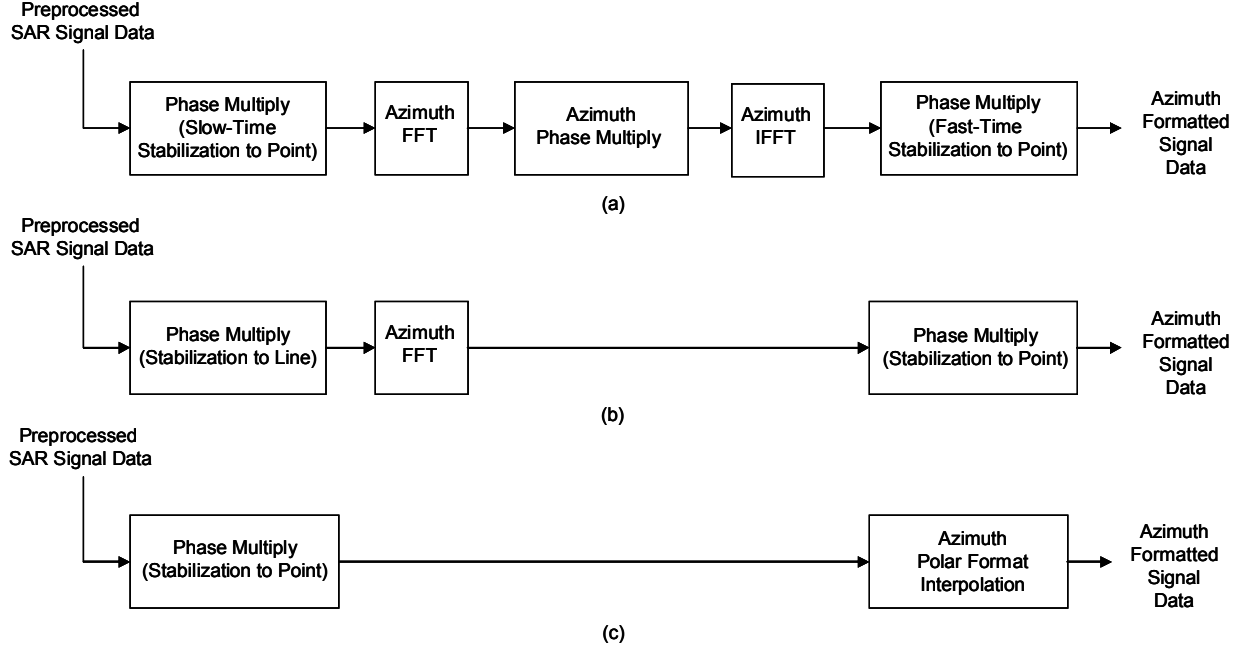
Fig. 5. Comparison of azimuth channel signal flows. (a) ATAFS for DDA. (b) RMA. (c) Conventional PFA.

A. ATAFS for WPFA and SPA

Within ATAFS for WPFA and SPA, the first step of data stabilization removes the quadratic component of the azimuth chirp associated with the received data from scene center. This azimuth chirp naturally varies with range frequency K_R and requires a 2-D phase multiply. This process resembles the data stabilization to a point associated with spotlight mode. However, it does not remove the higher order, non-quadratic components of azimuth chirp. Nor does it remove the small natural variation in azimuth chirp with target range.

The next operation is an azimuth Fourier transform. Because the preceding phase adjustment removes most of the azimuth chirp from all targets, the Fourier transform nominally compresses these signals in azimuth. The data now reside in the range frequency by azimuth image domain illustrated in Fig. 7a. Similar to the common range deskew operation, ATAFS now multiplies by a K_R-dependent azimuth quadratic phase function (illustrated by the quadratic curve in Fig 7a) to both migrate and scale the azimuth data support in a desirable fashion after the subsequent inverse azimuth Fourier transform. Fig. 6c illustrates this change in support that we explain below. This process does not accomplish azimuth polar formatting.

The azimuth location of each target's response in Fig. 7a determines the coefficient of the nearly linear phase it receives from the quadratic phase multiply. For example, scene center point A receives no linear phase because it is located at the azimuth origin. However, right azimuth point C receives a large linear phase because it is offset in azimuth. This azimuth-dependent difference in linear phase causes an azimuth-dependent shift in the 2-D phase history support following the azimuth inverse FFT of ATAFS processing. Data support boxes A and C in Fig. 6c indicate this shift.

Similarly, the width of each target's response in azimuth determines the amount of quadratic phase it accrues from the quadratic phase multiply. For example, far range point B has a slightly defocused impulse response in azimuth because its range offset in the scene causes its original azimuth chirp to be smaller than that of scene center. Because its response is defocused in azimuth, point B accrues a larger quadratic phase over its support than does point A. This extra quadratic phase causes a range-dependent scaling of the 2-D data support after the subsequent inverse FFT in ATAFS. The width of support box B relative to box A in Fig. 6c indicates this scaling.

The final ATAFS phase adjustment (the second step of data stabilization) in Fig. 4a removes the residual phase left from the quadratic functional form of the initial data stabilization. This adjustment completes the process of data stabilization to a fixed reference point at the output of ATAFS.

B. ATAFS for DDA

Within ATAFS for DDA, the first step of data stabilization removes the quadratic component of the azimuth chirp associated with the radar data received from scene center at the center transmitted frequency. This operation consists of a pulse-by-pulse phase shift with no dependence on radial frequency. It resembles the common data stabilization to a point associated with spotlight mode, but removes neither the differential Doppler across the transmitted bandwidth nor the higher order, non-quadratic components of the azimuth chirp. The next operation is an azimuth Fourier transform. Because the preceding phase adjustment approximately removes the azimuth chirp from all targets only for the center transmitted frequency, the Fourier transform nominally compresses these signals in azimuth at center frequency only and spreads the data out in an hourglass shape indicative of the differential Doppler
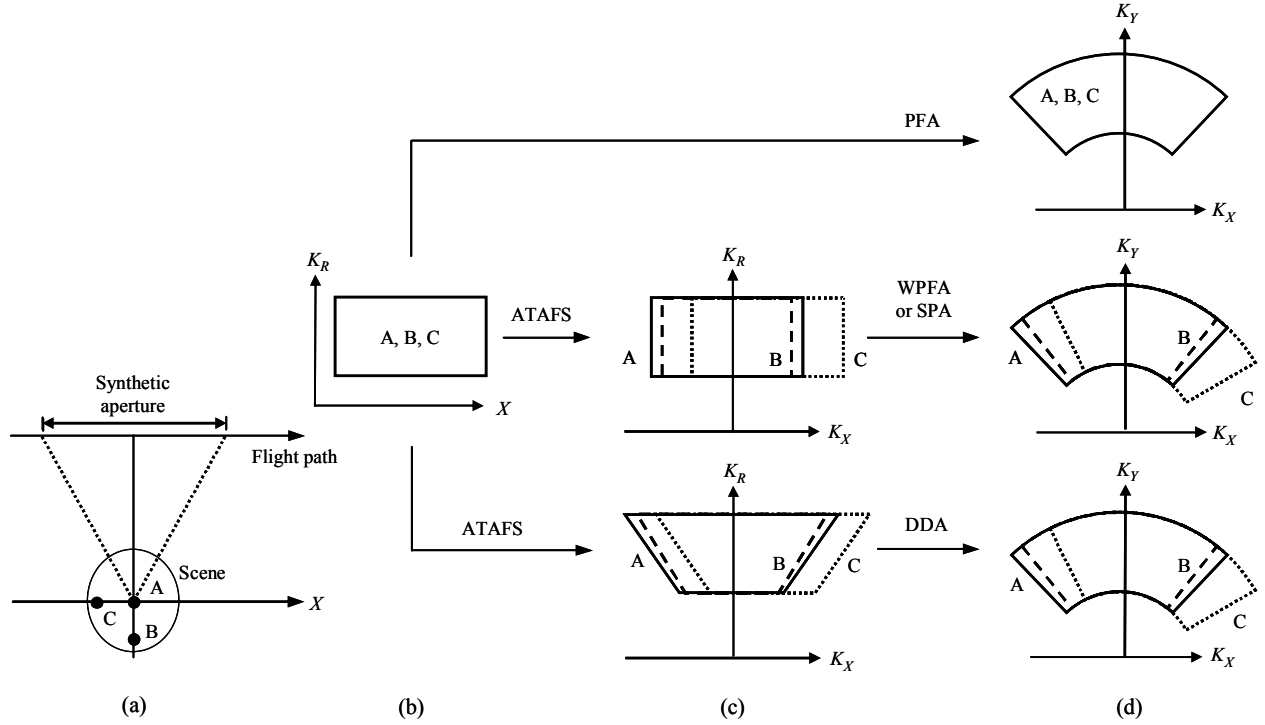
Fig. 6. Data support for three targets using PFA in upper row, WPFA or SPA in middle row, and DDA in lower row. (a) Data collection geometry. (b) Support after range deskew. (c) Support after ATAFS. (d) Support after final formatting.

bandwidth over the full range bandwidth. The data now reside in the range frequency by azimuth image domain illustrated in Fig. 7b. ATAFS now multiplies by an azimuth quadratic phase function that is independent of K_R to migrate, scale, and polar format the azimuth data support in a desirable fashion after the subsequent inverse azimuth Fourier transform.

As in the case of WPFA, the azimuth location of each target's response determines the coefficient of the nearly linear phase it receives from the quadratic phase multiply and appropriately shifts the 2-D phase history support in azimuth after an azimuth inverse FFT. Likewise, the width of each target's response in azimuth determines the amount of quadratic phase it accrues from the quadratic phase multiply and causes a range-dependent scaling of the 2-D data support after the subsequent inverse FFT. In this case, the scaling varies with radial frequency to achieve naturally the desired azimuth flaring associated with azimuth polar formatting. Data support boxes A, B, and C in Fig. 6c indicate this shift, scaling, and flaring for each target.

This variation in scaling with radial frequency occurs because ATAFS (for DDA) does not vary its azimuth quadratic phase adjustment as a function of K_R in the initial data stabilization operation. The differential Doppler bandwidth as a function of K_R adds azimuth bandwidth to the hourglass data at high K_R and subtracts bandwidth at low K_R. The presence of this differential bandwidth introduces the azimuth flaring of the data support. The final ATAFS phase adjustment in Fig. 4a accounts for the phase effects associated with this differential Doppler to complete the process of data stabilization to a fixed reference point at the output of ATAFS.

C. Data Support after ATAFS

Fig. 6 illustrates the 2-D phase history support of three point targets at different locations within a spotlight scene during PFA, WPFA, SPA, and DDA image formation. In spotlight mode, the collected phase history from each target occupies the same support in (X, K_R) space as Fig. 6b illustrates. The upper branch of Fig. 6d shows the conventional PFA in which all targets in the scene receive a common format modification and have identical support in the formatted phase history. Fig. 2b illustrates this PFA result in a similar way.

The middle branch of Fig. 6 illustrates data support after ATAFS completes along-track scaling and shifting and after final WPFA or SPA processing achieves the appropriate polar storage format. The lower branch shows DDA processing in which ATAFS processing achieves the necessary along-track scaling, shifting, and flaring of the signals before Stolt interpolation establishes the needed range formatting. These results achieve the ideal format for all targets that Fig. 2c illustrates in a similar way.

D. Image Quality Performance

We have evaluated the performance of three ATAFS-based algorithms against simulated SAR phase histories representing a stressful combination of imaging geometry and radar system parameters. For this simulation, the center frequency was 242MHz, the scene size was 0.5×0.5km, the standoff range was 1km, and processed resolution was 1×1m. We simulated SAR data from an array of point targets in a rectangular pattern to evaluate geometric distortion and image focus. Fig. 8 shows
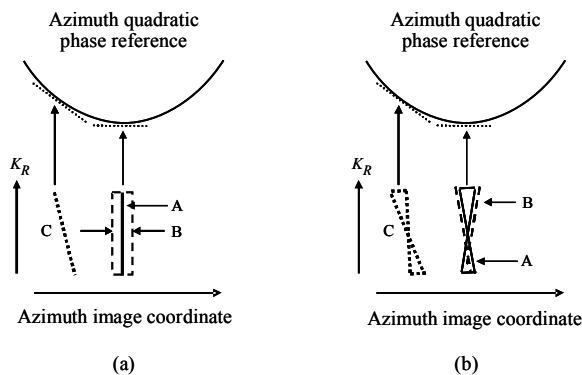
Fig. 7. Application of ATAFS quadratic phase multiply. (a) Use in WPFA and SPA. (b) Use in DDA.

the image that results from PFA processing. Both geometric distortion and the spatially-variant azimuth defocusing of targets caused by uncompensated RCQPE are evident. Fig. 9 shows the image that results from using WPFA to process the same SAR data. This image is focused well and has no geometric distortion. Near range is at the top in these images. A comparison of the image in Fig. 9 with a similar result (not shown) using RMA processing indicates that both algorithms yield identical image quality. Likewise, processing this data via SPA or DDA produces the same image quality also.

IV. SUMMARY

The new widefield algorithms have the potential to generate large-scene, fine-resolution images in all SAR modes. They operate in both broadside and squinted data collection geometries. They can produce a large image using a single processing batch without subdividing the input data or the imaged scene. Their output imagery is naturally without geometric distortion and contains no residual phase errors associated with range curvature. They achieve these ideal attributes because they format the data from each scatterer within a scene into the ideal data format for that scatterer.

An attractive implementation of WPFA uses ATAFS as a preprocessing adjunct to an existing PFA processor. The WPFA configuration removes the range curvature phase errors present in PFA to produce fully-focused, widefield imagery without geometric distortion. The SPA variation of WPFA achieves identical data formatting with Stolt interpolation following azimuth interpolation rather than the azimuth interpolation following range interpolation typical of PFA processors.

The DDA consists of ATAFS, an azimuth parameter scaling step that requires no signal processing operations, and conventional Stolt interpolation. It operates on data dechirped in range and azimuth to achieve ideal azimuth formatting without azimuth interpolation. This processor configuration is mathematically equivalent to RMA and produces fully-focused, widefield imagery without geometric distortion.

REFERENCES

[1] Cafforio, C., C. Prati, and F. Rocca, "SAR Data Focusing Using Seismic Migration Techniques," *IEEE Transactions on Aerospace and Electronic Systems*, Vol. 27, No. 2, March 1991, pp. 194-206.

[2] Carrara, W.G., R.S. Goodman, R.M. Majewski, *Spotlight Synthetic Aperture Radar: Signal Processing Algorithms*, Norwood, MA, Artech House, 1995.

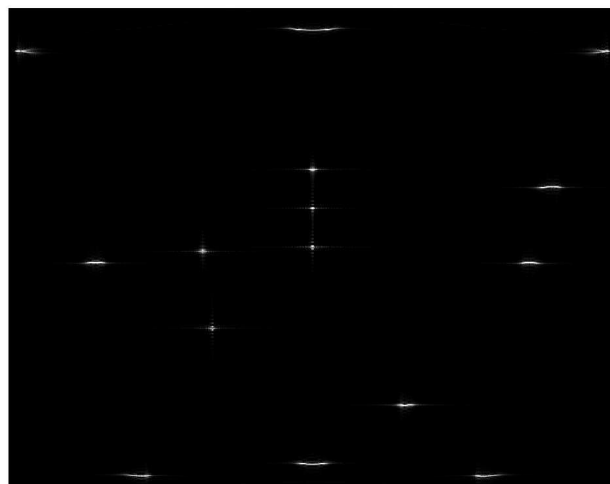[3] Stolt, R.H., "Migration by Fourier Transform," *Geophysics*, Vol. 43, No. 1, February 1978, pp. 23-48.
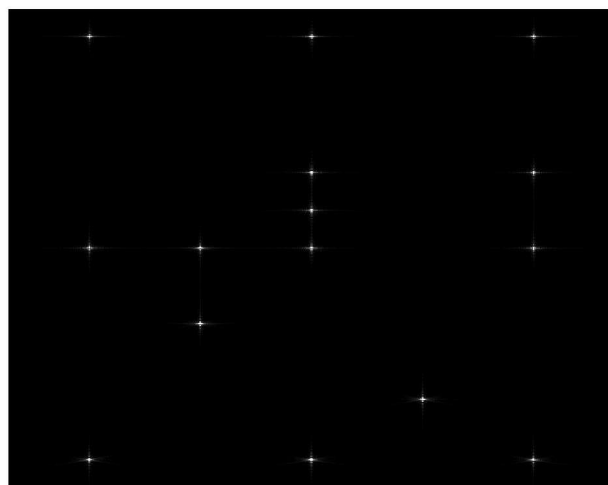
Fig. 8. PFA image.

Fig. 9. WPFA image.